Design of DGT-based Linear Receivers for GFDM Transmission in Broadband Channels

Francesco Linsalata[1], Atul Kumar[2], Maurizio Magarini[1]
[1]Dipartimento di Elettronica, Informazione e Bioingegneria, Politecnico di Milano, Italy,
[2] Vodafone Chair Mobile Communications Systems, Technische Universität Dresden, Germany.
Email: francesco.linsalata@mail.polimi.it

***Abstract*— Generalized frequency-division multiplexing (GFDM) is a non orthogonal multicarrier transmission scheme proposed for future generation wireless networks. Due to its attractive properties, it could fulfill the requirements of future scenarios. Although its characteristics and performance have been analyzed in many previous works, there is still room for improvement in some aspects. This paper deals with the design of receivers for GFDM transmission over a frequency selective channel. Linear equalization schemes, such as zero-forcing and minimum mean-squared error, are developed to decide the transmitted symbols. For the derivation we rely on the discrete Gabor transform (DGT) interpretation of GFDM, when the synthesis function, *i.e.*, the pulse shaping filter, and the analysis function, *i.e.*, the receiving filter, satisfy the *Wexler-Raz* identity. Choosing functions that satisfy the Wexler-Raz condition allows for optimal symbol-by-symbol detection for a DGT-based receiver in case of transmission over an ideal channel. However, when transmission takes place over a frequency selective channel symbol-by-symbol detection is not longer optimal due to inter-sub-symbol interference generated by sub-symbols transmitted on the same sub-carrier. Monte Carlo simulations are used to show the symbol error rate performance achieved with the proposed design for linear receivers based on DGT interpretation of GFDM.**

I. Introduction

In the fifth generation (5G) and beyond 5G (B5G) networks, the scenarios foreseen will require very high spectral efficiency, relaxed synchronization, very low latency, and low out-of-band (OOB) emission. The look for new waveforms that are able to support variable and customizable pulse shaping filters is therefore one of the research priorities in order to achieve a better trade-off between time-domain and frequency-domain localization [1], [2]. A main characteristic is the flexibility to support mixed services with different waveform parameters within one carrier, which is a key requirement in the physical layer of future cellular networks [3]–[6].

With this aim, generalized frequency division multiplexing (GFDM), which is based on the use of circular filtering at sub-carrier level, was proposed as a new multicarrier modulation scheme [7], [8]. Compared to orthogonal frequency-division multiplexing (OFDM), the main advantages of GFDM consist in a reduction of the OOB emission, achieved by means of filtering at sub-carrier level [5], and in an increase of the spectral efficiency, obtained through the introduction of tail biting, which makes the length of the cyclic prefix (CP) independent from that of pulse shaping filter [9], [10]. Moreover, the flexible frame structure of GFDM allows, by changing the number of time slots and of sub-carriers in a frame, covering both conventional OFDM and discrete Fourier transform (DFT) spreaded OFDM (DFT-s-OFDM), which results in complete backward compatibility with long-term evolution (LTE) and advanced LTE [9].

Radio access technologies for cellular mobile communications are typically characterized by multiple access schemes. Among these orthogonal frequency-division multiple access (OFDMA) was a reasonable choice for achieving good system level throughput performance in packet-domain services with single user detection. The engineering community witnessed the development of wide radio bands such as the millimeter-waves (mm-waves) frequencies to fulfill the explosive growth of mobile data demand and pave the way towards 5G networks [14]. As a result, the introduction of new advanced multicarrier modulation techniques and the use of massive multiple-input multiple-output (MIMO) systems are considered as a means to increase the spectral efficiency, thus achieving higher data rates. The use of ultra-broadband pulses, just a few hundred femtoseconds long, has been recently proposed [15]. Moreover, energy efficiency and high data rate are some of the key advantages driving much of the interest in the novel THz massive MIMO systems for the new network paradigm. The high peak-to-average power ratio (PAPR) of the OFDM works against this advantages and can impede good downlink and uplink performance [16]. In contrast, the additional degree of freedom from the adjustable sub-carrier filters in GFDM allows further control of the PAPR [17] and several advantages of GFDM have been already brought to MIMO application without increasing the system complexity [18].

Despite the above mentioned advantages, a main issue of GFDM compared to OFDM is the need of equalization, implemented by block-based processing in time or frequency domain, that is required even in the case of transmission over an ideal channel [8]. For an efficient implementation of the GFDM receiver in time-domain, a relationship between GFDM signal and discrete Gabor transform (DGT) was proposed in [11]. It was shown that GFDM transmission and reception are equivalent to a finite discrete Gabor expansion and DGT in critical sampling, respectively. The Gabor interpretation allows an optimal symbol-by-symbol detector, after the DGT-based receiver, when transmisison takes place over an ideal channel. An equivalent interpretation of the DGT receiver in frequency-domain was given in [12], which allows for signal

recovery with lower complexity compared to the time-domain approach.

However, it is worth observing that when transmission over a frequency-selective channel is considered the DGT interpretation with critical sampling looses its validity. In this case, to restore the condition required for using DGT at the receiver, the effect of the channel must be taken into account in the equalization of the whole GFDM symbol. This aspect was considered in [12], where it was observed that the performance of the proposed low complexity frequency-domain equalization approach for the DGT-based GFDM system was close to that of OFDM only when the number of sub-symbols transmitted on each sub-carrier is low. When this number increases the resulting signal-to-interference ratio is much lower than that of OFDM with a rapid degradation in the performance. This degradation of performance is due to the inter-sub-symbol interference (ISSI) that arises from the sub-symbols transmitted with the same sub-carrier, which is not properly considered in [12]. The main contribution of this paper consists in the definition of a model for the received signal and in the design of time-domain receivers that operate on a subcarrier basis by counteracting ISSI, which allows evaluation of the best strategy for the detection of transmitted symbols according to the desired performance and degree of complexity. In particular, we will focus on the design of linear equalization schemes, such as zero-forcing (ZF) and minimum mean-squared error (MMSE).

The structure of the paper is as follows. In Sec. II we will introduce the DGT interpretation of GFDM. The design of the different types of linear receivers will be considered in Sec. III. Section IV will present the results of Monte Carlo simulations and, finally, conclusion will be drawn in Sec. V.

II. DGT-BASED GFDM SYSTEM MODEL

With reference to one GFDM symbol, the block of transmitted bits is applied to the input of a mapper that gives at its output an $M \times K$ data matrix $\mathbf{X}$ whose $N = MK$ elements take values from a complex constellation, *e.g.*, phase-shift keying [10]. The data matrix $\mathbf{X}$ is sent to the GFDM modulator, based on K sub-carriers, where each sub-carrier is used to transmit M sub-symbols. According to this model the data matrix $\mathbf{X}$ can be represented as the composition of K column vectors

$$\mathbf{X} = [\mathbf{X}_0, \mathbf{X}_1, \cdots, \mathbf{X}_{K-1}], \tag{1}$$

where

$$\mathbf{X}_k = [X_k(0), X_k(1), \cdots, X_k(M-1)]^T, \tag{2}$$

with $X_k(m)$ representing the mth sub-symbol, $m = 0, \ldots, M-1$, transmitted on the kth sub-carrier, $k = 0, \ldots, K-1$ and $(\cdot)^T$ denoting the transposition operation. The time-duration of each symbol vector $\mathbf{X}_k$ is MT_s with sub-carrier spacing equal to $1/(MT_s)$, T_s being the symbol interval on each sub-carrier. The M sub-symbols of the kth group are upsampled by a factor K and applied to the input of a periodic pulse shaping filter with N coefficients. After pulse shape filtering, the nth sample of the transmitted GFDM signal is written as

$$x(n) = \sum_{k=0}^{K-1} \sum_{l=0}^{M-1} X_k(l) g_{k,l}[n] = \sum_{k=0}^{K-1} \sum_{l=0}^{M-1} X_k(l) g[\langle n - lK \rangle_N] \, e^{\frac{j2\pi kn}{K}}, \tag{3}$$

where $n = 0, 1, \cdots, N-1$, is the sampling index and $\langle \cdot \rangle_N$ denotes the modulo N operation that implements the circular shifting of the periodic prototype discrete-time impulse response $g[n]$ of length N.

A. Transmission over an Ideal Channel

As first observed in [11], equation (3) can be interpreted as an inverse DGT (IDGT), where $g[n]$ represents the synthesis function whose time-domain translations and frequency-domain shiftings $g_{q,m}[n]$ are weighted by transmitted symbols. With this interpretation, in case of transmission over an ideal channel the symbols $X_q(m)$ can be recovered from $x(n)$ at the receiver by applying DGT as

$$X_q(m) = \sum_{n=0}^{N-1} \gamma^*_{q,m}[n] x(n), \tag{4}$$

where $\gamma_{q,m}$ is a periodic discrete function with period N, which is defined as the analysis function obtained from time and frequency shifts of an analysis window $\gamma[n]$ as

$$\gamma_{q,m}[n] = \gamma[\langle n - mK \rangle_N] \, e^{\frac{j2\pi qn}{K}}. \tag{5}$$

Note that, the identity defined by (4) holds only when the synthesis function $g[n]$ and the analysis function $\gamma[n]$ satisfy the *Wexler-Raz* identity given in [12, eq. (11)]. If this condition is not satisfied interference arises both from symbols transmitted on other sub-carriers and from sub-symbols transmitted with the same sub-carrier.

B. Transmission over a Frequency-selective Channel

When transmission takes place over a frequency-selective channel, the effect of inter-symbol interference introduced by the time spread of the channel can be mitigated by inserting a CP, which consists of N_{CP} samples such that the length of the CP is at least equal to the length of the channel. The CP-extended signal is written as

$$\tilde{x}(n) = \begin{cases} x(N+n), & n = -N_{CP}, \ldots, -1, \\ x(n), & n = 0, \ldots, N-1. \end{cases} \tag{6}$$

We consider here the same L-path tapped delay line channel model defined in [13]. According to this model, the continuous-time impulse response of the multi-path fading channel is defined as

$$h(t) = \sum_{i=0}^{L-1} h_i \delta(t - \tau_i), \tag{7}$$

where h_i is the complex amplitude, *i.e.*, tap coefficient, of the ith path associated with the propagation delay τ_i and $\delta(t)$ is the delta Dirac function. When $L = 1$ we get the flat fading Rayleigh channel model. For the particular case where h_0 is constant and equal to 1 we have the ideal channel.

In the following, for simplicity, we consider the case where $\tau_i = i$, with $i = 0, \ldots, L-1$. The tap coefficients h_i, $i = 0, 1, 2, \ldots, L-1$, are modeled as independent and identically distributed zero mean complex random variables with average power $\sigma_i^2 = 1/L$, uniform distributed phase in $[0, 2\pi)$, and Rayleigh distributed amplitude. According to such a model we have $\sigma_0^2 + \sigma_1^2 + \cdots + \sigma_{L-1}^2 = 1$.

After passing through the channel the received signal is written as

$$y(n) = \sum_{i=0}^{L-1} h_i \tilde{x}(n-i) + w(n), \tag{8}$$

where $w(n)$ represents the complex AWGN with zero mean and variance N_0 per dimension. Under the assumption $N_{CP} \geq L-1$, by removing the effect of the cyclic prefix and by replacing (3) in (8) we get

$$y(n) = \sum_{i=0}^{L-1} h_i \sum_{k=0}^{K-1} \sum_{l=0}^{M-1} X_k(l) g[\langle n-i-lK \rangle_N] \, e^{\frac{j2\pi k(n-i)}{K}} + w(n). \tag{9}$$

In order to recover the transmitted symbols, the DGT defined in (4) is applied to the received signal as

$$\begin{aligned} Y_q(m) &= \sum_{n=0}^{N-1} \gamma_{q,m}^*[n] y(n) = \sum_{n=0}^{N-1} \gamma^*[\langle n - mK \rangle_N] \, y(n) \, e^{-\frac{j2\pi qn}{K}} \\ &= \sum_{k=0}^{K-1} \sum_{l=0}^{M-1} X_k(l) \sum_{i=0}^{L-1} h_i P_{(q-k)M}[(m-l)K, i] e^{-\frac{j2\pi ki}{K}} + W_q(m), \end{aligned} \tag{10}$$

where $W_q(m)$ is the DGT of the AWGN and

$$\begin{aligned} P_{kM}[l,i] &= \sum_{n=0}^{N-1} \gamma^*[n] \, g[\langle n - i + lK \rangle_N] \, e^{-\frac{j2\pi kn}{K}} \\ &= \frac{1}{N} \sum_{q=0}^{N-1} \Gamma_q^* G_{\langle q+kM \rangle_N} e^{-\frac{j2\pi(q+kM)(i-lK)}{N}} \\ &= \left(\frac{1}{N} \sum_{q=0}^{N-1} \Gamma_q^* G_{\langle q+kM \rangle_N} e^{\frac{j2\pi ql}{M}} e^{-\frac{j2\pi qi}{N}} \right) e^{-\frac{j2\pi ki}{K}} \end{aligned} \tag{11}$$

with Γ_q and G_q corresponding to the N-points DFT of $\gamma[n]$ and $g[n]$, respectively.

As a function satisfying the Wexler-Raz identity with critical sampling in what follows we consider a Dirichlet pulse, also referred *discrete sinc*, which is characterized by a DFT that is a rectangular pulse

$$G_k^D = \begin{cases} 1, & \left(0 \leq k \leq \lceil \frac{M}{2} \rceil - 1\right) \bigcup \left(N - \lfloor \frac{M}{2} \rfloor \leq k \leq N-1\right), \\ 0 & otherwise, \end{cases} \tag{12}$$

where $\lceil \cdot \rceil$ and $\lfloor \cdot \rfloor$ denote the nearest upper and lower integer, respectively. With the use of Dirichlet function we have $\gamma[n] = g[n]$, and the filtering implemented at the receiver with the analysis function $\gamma[n]$ can be therefore interpreted as satisfying the matched and ZF condition at the same time. By setting $G_k = G_k^D$ in (11) we get

$$P_{kM}[lK, i] = \delta[k] \frac{1}{N} \frac{\sin(\frac{\pi(i-lK)}{K})}{\sin\left(\frac{\pi(i-lK)}{N}\right)} e^{\frac{j\pi(i-lK)(1+(-1)^M)}{2N}}, \tag{13}$$

where $\delta[k]$ denotes the Kronecher delta. In the special case $i = 0$, (13) converts into eq. (14) of [12], for which we obtain the Wexler-Raz identity

$$\begin{aligned} P_{kM}[lK, 0] &= \frac{1}{N} \sum_{q=0}^{N-1} \Gamma_q^* G_{\langle q+kM \rangle_N} e^{\frac{j2\pi ql}{M}} = \delta[k]\delta[l], \\ &0 \leq k \leq K-1, \text{ and } 0 \leq l \leq M-1. \end{aligned} \tag{14}$$

By substituting $P_{kM}[lK, i]$ given in (13) into (10), after some mathematical manipulation (10) can we rewritten as

$$\begin{aligned} Y_q(m) &= \sum_{l=0}^{M-1} X_q(l) \sum_{i=0}^{L-1} h_i \frac{\sin\left(\frac{\pi(i-(m-l)K)}{K}\right)}{\sin\left(\frac{\pi(i-(m-l)K)}{N}\right)} e^{\frac{-j2\pi qi}{K}} + W_q(m) \\ &= \sum_{l=0}^{M-1} X_q(l) \bar{H}_{qM}((m-l)K) + W_q(m), \end{aligned} \tag{15}$$

where the even property of the periodic Dirichlet sinc function has been used. The above equation shows that in case of Dirichlet function the interference is generated only by sub-symbols transmitted on the same sub-carrier and not from sub-symbols transmitted on other sub-carriers. The "windowed" channel is given by

$$\bar{H}_q(m) = \sum_{i=0}^{N-1} h_i^{(ZP)} w_{\langle i-m \rangle_N} e^{\frac{-j2\pi qi}{N}}, \tag{16}$$

where $w_{\langle i-m \rangle_N}$ corresponds to a shifting of m samples of the periodic windowing function

$$w_n = \frac{\sin\left(\frac{\pi n}{K}\right)}{\sin\left(\frac{\pi n}{N}\right)}, \qquad n = 0, \ldots, N-1, \tag{17}$$

and

$$h_i^{(ZP)} = \begin{cases} h_i & i = 0, \ldots, L-1, \\ 0 & i = L, \ldots, N-1. \end{cases} \tag{18}$$

Equation (16) can be rewritten as

$$\bar{H}_q(m) = H_q \otimes_N W_q e^{-j\frac{2\pi mq}{N}}, \tag{19}$$

which is the circular convolution between the DFT of the channel and the DFT of the shifted windowing function, where $W_q = G_q^D$. According to the definition of G_k^D given in (12), eq. (19) realizes a weighted average of M frequency domain values of H_k around $k = q$, where the weights are obtained from the complex exponential for a given m. The M samples H_k involved in the average are $k = \langle q - \lfloor \frac{M}{2} \rfloor, \ldots, q-1 \rangle_N$ and $k = \langle q, \ldots, q + \lceil \frac{M}{2} \rceil - 1 \rangle_N$, which define the M points around q taking into account of the periodic nature of H_k. After some straightforward mathematical manipulations, (10) can be rewritten as

$$Y_q(m) = \underbrace{X_q(m)\bar{H}_{qM}(0)}_{\substack{m\text{th sample received} \\ \text{on the } q\text{th sub-carrier}}} + \underbrace{\sum_{l=0, l\neq m}^{M-1} X_q(l)\bar{H}_{qM}((m-l)K)}_{\substack{\text{Interference induced by sub-symbols} \\ \text{other than } X_q(m) \text{ transmitted} \\ \text{on the } q\text{th sub-carrier}}} + \underbrace{W_q(m)}_{\text{AWGN Noise}}, \tag{20}$$

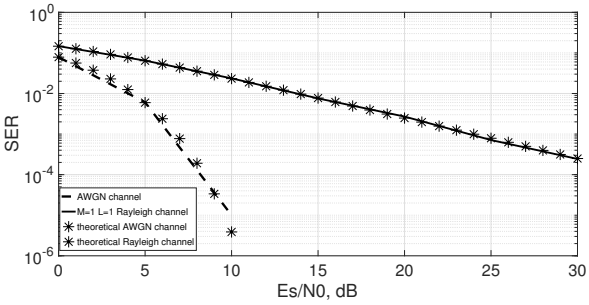

Fig. 1. Theoretical and simulated with MMSE receiver SER vs. E_s/N_0 of the DGT-based GFDM in special case of BPSK transmission over a flat Rayleigh fading channel and AWGN channel with $L = 1$ and $M = 1$.

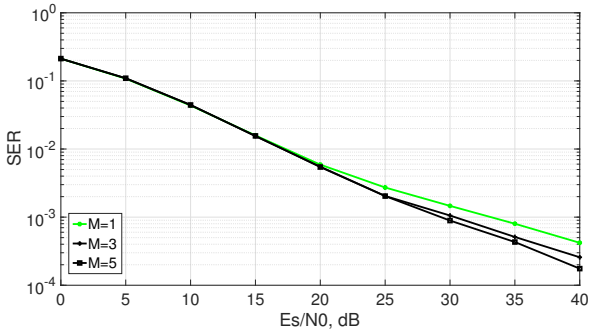

Fig. 2. SER vs. E_s/N_0 for the DGT-based GFDM with ZF receiver in case of BPSK transmission over frequency selective Rayleigh fading channel with $L = 2$ and $K = 16$ for different value of M.

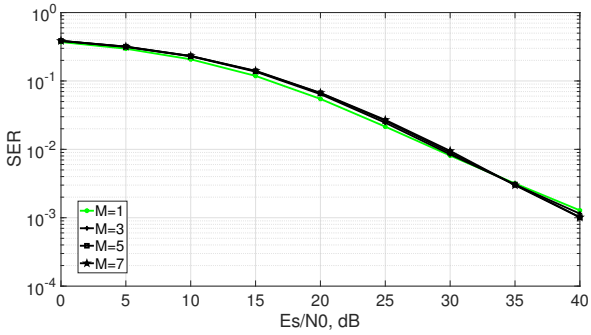

Fig. 3. SER vs. E_s/N_0 for the DGT-based GFDM with ZF receiver in case of BPSK transmission over frequency selective Rayleigh fading channel with $L = 9$ and $K = 16$ for different value of M.

where it appears that the mth sub-symbol transmitted on the qth sub-carrier $X_q(m)$ is

- scaled by the term $\bar{H}_{qM}(0)$;
- impaired by the interference generated by the mth sub-symbol transmitted on the same sub-carrier through the term $\bar{H}_{qM}(l-m)K$, $l \neq m$;
- distorted by the AWGN term $W_q(m)$.

III. Design of Linear Receivers

With reference to (20), we define the vector of the received signal $\mathbf{Y}_q = [Y_q(0), Y_q(1), \ldots, Y_q(M-1)]^T$ on the qth sub-carrier, which is given by

$$\mathbf{Y}_q = \bar{\mathbf{H}}_{qM}\mathbf{X}_q + \mathbf{W}_q, \qquad q = 1, \ldots, K-1, \tag{21}$$

where $\mathbf{W}_q = [W_q(0), W_q(1), \ldots, W_q(M-1)]^T$ and

$$\bar{\mathbf{H}}_{qM} = \begin{bmatrix} \bar{H}_{qM}(0) & \bar{H}_{qM}(N-K) & \cdots & \bar{H}_{qM}(N-(M-1)K) \\ \bar{H}_{qM}(N-(M-1)K) & \bar{H}_{qM}(0) & \cdots & \bar{H}_{qM}(N-K) \\ \vdots & \vdots & \ddots & \vdots \\ \bar{H}_{qM}(N-K) & \bar{H}_{qM}(N-2K) & \cdots & \bar{H}_{qM}(0) \end{bmatrix}. \tag{22}$$

It is worth noting that the model in (21) is the same as that used to describe the received vector in a MIMO system [19]. With this interpretation it is possible to design several type of receivers according to the desired trade-off between performance and complexity.

Here, we consider linear receivers schemes to take a decision on the transmitted vector. For such a class of receivers an estimate of the M sub-symbols transmitted on the q sub-carrier is obtained by linear weighting the received vector as

$$\hat{\mathbf{X}}_q = \mathbf{C}_{qM}\mathbf{Y}_q. \tag{23}$$

Then, a threshold detector is used to decide independently the M symbols. The linear weighting matrix $\mathbf{C}_{qM}$ can be designed both by using ZF and MMSE criteria [20]. The details of each receiver are describe below:

- **ZF Receiver** removes the ISI at the receiver, but with the possible noise enhancement that decreases the SNR. For the ZF receiver the expression of the demodulation matrix is given by

$$\mathbf{C}_{qM,\mathrm{ZF}} = (\bar{\mathbf{H}}_{qM}^H\bar{\mathbf{H}}_{qM})^{-1}\bar{\mathbf{H}}_{qM}^H, \tag{24}$$

  where ^{H} denotes Hermitian transpose conjugation.
- **MMSE Receiver** gives a trade-off between noise enhancement and ISI. The expression of the demodulation matrix is

$$\mathbf{C}_{qM,\mathrm{MMSE}} = (\bar{\mathbf{H}}_{qM}^H\bar{\mathbf{H}}_{qM} + N_0\mathbf{I}_\mathbf{M})^{-1}\bar{\mathbf{H}}_{qM}^H, \tag{25}$$

  where N_0 is the variance of the noise and $\mathbf{I}_M$ is an $M \times M$ identity matrix.

IV. Simulation Results

The performance of the proposed design is evaluated by means of Monte Carlo simulations for $K = 16$ and different lengths of the frequency selective Rayleigh fading channel model defined in Sec. II. Figure 1 reports Monte Carlo simulations and theoretical results of the symbol error rate (SER) versus SNR for GFDM transmission when BPSK symbols are transmitted over an AWGN channel and a flat Rayleigh fading channel. From these results it is evident that GFDM based on DGT interpretation has the same theoretical performance as that of BPSK in case of transmission over non-frequency selective channels. Figures 2 and 3 show the SER versus E_s/N_0 achieved by the ZF linear receiver with $L = 2$ and $L = 9$, respectively, and different values of M. It is worth observing that when $M = 1$ we get the conventional OFDM system. For both the two considered lengths it can be seen

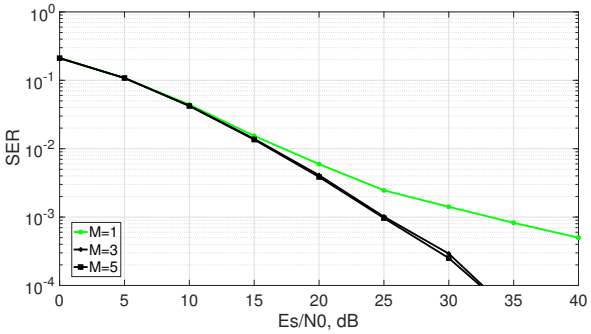

Fig. 4. SER vs. E_s/N_0 for the DGT-based GFDM with MMSE receiver in case of BPSK transmission over frequency selective Rayleigh fading channel with $L = 2$ and $K = 16$ for different value of M.

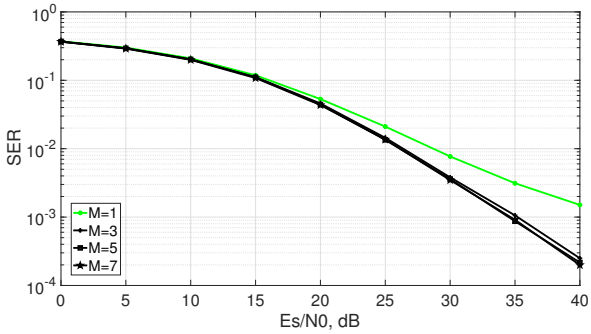

Fig. 5. SER vs. E_s/N_0 for the DGT-based GFDM with MMSE receiver in case of BPSK transmission over frequency selective Rayleigh fading channel with $L = 9$ and $K = 16$ for different value of M.

that the performance is almost the same for all the considered values of M. However, for $L=2$ it can be observed that at values of SNR greater than 20 dB there is performance gain for $M=3,5$ compared to $M=1$, which is due to a change in the slope of the curve. The change of slope is more evident when MMSE linear detection is considered in place of ZF linear detection since it starts at lower SNR values. This can be observed in Figs. 4 and 5 where the results obtained for MMSE linear detection are reported for the same channel lengths and values of M considered for ZF linear detection. As expected, the linear MMSE offers a superior performance compared to linear ZF, which is more consistent for $L=9$ than for $L=2$. For both the two considered lengths it can be seen that for $M>1$ a higher improvement of performance is achieved.

V. Conclusion

In this paper the optimal per-subcarrier design of time-domain MMSE and ZF linear receivers for GFDM transmission over a frequency selective channel is proposed. The approach, which relies on the DGT interpretation of GFDM, is based on the modelling of the inter-sub-symbol interference among sub-symbols transmitted on the same sub-carrier when the Dirichlet function is used as pulse shaping filter. The SER performance achived by ZF and MMSE is evaluated by means of Monte Carlo simulations. Compared to the OFDM case a performance improvement is observed for increasing number of sub-symbols transmitted on the same sub-carrier, which is due to a steep decreasing slope of the SER curve as SNR increases.

References

[1] Y. Cai, Z. Qin, F. Cui, G. Y. Li and J. A. McCann, "Modulation and multiple access for 5G networks," *IEEE Comm. Sur. Tut.*, vol. 20, no. 1, pp. 629–646, Mar. 2018.

[2] X. Zhang *et al.*, "On the waveform for 5G," *IEEE Commun. Mag.*, vol. 54, no. 11, pp. 74–80, Nov. 2016.

[3] T. Taleb and A. Kunz, "Machine type communications in 3GPP networks: potential, challenges, and solutions," *IEEE Comm. Mag.*, vol. 50, no. 3, pp. 178–184, March. 2012.

[4] A. A. Zaidi *et al.*, "Waveform and numerology to support 5G services and requirements," *IEEE Commun. Mag.*, vol. 54, pp. 90–98, Nov. 2016.

[5] G. Wunder, *et al.*, "5GNOW: non-orthogonal, asynchronous waveforms for future mobile applications," *IEEE Commun. Mag.*, vol. 52, no. 2, pp. 97–105, Feb. 2014.

[6] P. Schulz, *et al.*, "Latency critical iot applications in 5G: perspective on the design of radio interface and network architecture," *IEEE Commun. Mag.*, vol. 55, no. 2, pp. 70–78, Feb. 2017.

[7] C. J. Zhang *et al.*, "New waveforms for 5G networks," *IEEE Commun. Mag.*, vol. 54, no. 11, pp. 64–65, Nov. 2016.

[8] N. Michailow *et al.*, "Generalized frequency division multiplexing for 5th generation cellular networks," *IEEE Trans. Comm.*, vol. 62, no. 9, pp. 3045–306, Sept. 2014.

[9] F. Schaich and T. Wild, "Waveform contenders for 5G: OFDM vs. FBMC vs. UFMC," in Proc. of *ISCCSP*, pp. 457-460, May 2014.

[10] A. Kumar and M. Magarini, "Improved Nyquist pulse shaping filters for generalized frequency division multiplexing," in Proc. of *LATINCOM*, pp. 1-7, Nov. 2016.

[11] M. Matthé, L. L. Mendes, and G. Fettweis, "Generalized frequency division multiplexing in a Gabor transform setting," *IEEE Commun. Lett.*, vol. 18, pp. 1379–1382, Aug. 2014.

[12] P. Wei, X. G. Xia, Y. Xiao, S. Li, "Fast DGT-based receivers for GFDM in broadband channels," *IEEE Trans. Commun.*, vol. 64, pp. 4331–4345, Oct. 2016.

[13] M. K. Simon and M.-S. Alouini, *Digital Communication over Fading Channels, 2nd ed.* New York: Wiley, 2005.

[14] H. Elayan, O. Amin, R. M. Shubair, M.-S. Alouini, "Terahertz communication: the opportunities of wireless technology beyond 5G," in Proc. of *IEEE CommNet*, 2018, pp. 1–5.

[15] J. M. Jornet and I. F. Akyildiz, "Femtosecond-long pulse-based modulation for terahertz band communication in nanonetworks," *IEEE Transactions on Communication*, vol. 62, no. 5, pp. 1742–1754, May 2014.

[16] S. Mumtaz, J. M. Jornet, J. Aulin, W. H. Gerstacker, X. Dong, "Terahertz communication for vehicular networks," *IEEE Transactions on Vehicular Technology*, vol. 66, no. 7, pp. 5617-5625, July 2017.

[17] N. Michailow and G. Fettweis, "Low peak-to-average power ratio for next generation cellular systems with generalized frequency division multiplexing," in Proc. of *IEEE International Symposium on Intelligent Signal Processing and Communication Systems*, 2013, pp. 651–655.

[18] E. Öztürk. E. Basar, H. A. Çırpan, "Spatial modulation GFDM: a low complexity MIMO-GFDM system for 5G wireless networks", in Proc. of *IEEE BlackSeaCom*, 2016, pp. 1–5.

[19] A. H. Mehana, A. Nosratinia, "Diversity of MMSE MIMO receivers," *IEEE Transactions on information theory*, vol. 58, no. 11, pp. 6788–6805, Nov. 2012.

[20] A. Paulraj, R. Nabar, D. Gore, "Introduction to space-time wireless communications," Cambridge, UK: Cambridge University Press, 2003.